Supplementary Information

Distinct loops in arrestin differentially regulate ligand binding in the GPCR opsin

Martha E. Sommer, Klaus Peter Hofmann, Martin Heck

Supplementary Figures

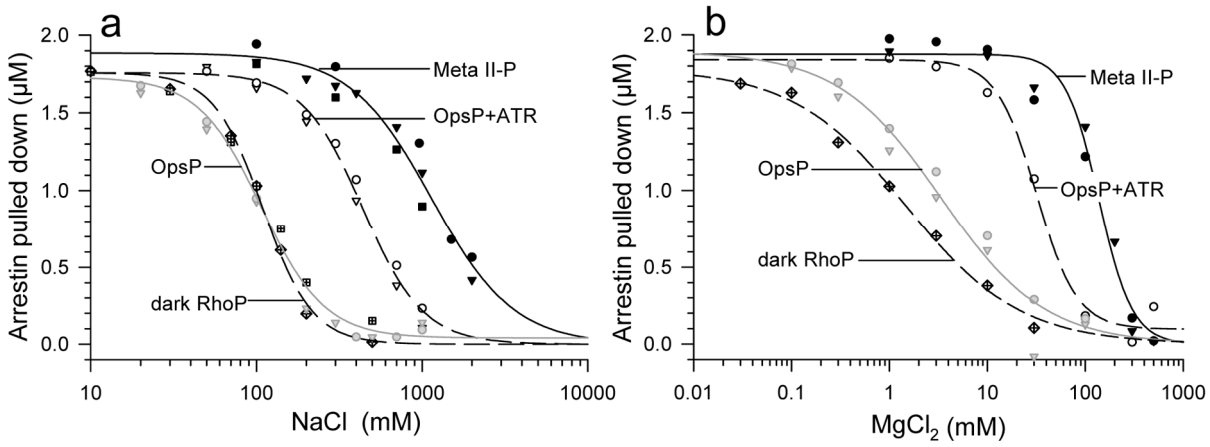

Supplementary Figure S1. Salt titrations against arrestin bound to different phosphorylated receptor species. (**a**) Arrestin (2 μM) binding to 8 μM Meta II-P (*black symbols*), 8 μM OpsP + 80 μM all-*trans*-retinal (ATR) (*white symbols*), 10 μM OpsP (*gray symbols*), or 20 μM dark-state RhoP (*crossed symbols*) was measured at increasing salt (NaCl) concentrations. Data points were fit as described in the *Methods*, and IC_{50} values are listed in Table S1. (**b**) The same as in (a), except that $MgCl_2$ was titrated against samples containing arrestin and different forms of the receptor. Arrestin binding was measured by the centrifugal pull-down assay employing fluorescently-labelled arrestin A366NBD. Data points from independent experiments are represented by differently shaped symbols, and the combined data points were used for curve fitting (see Supplementary Methods).

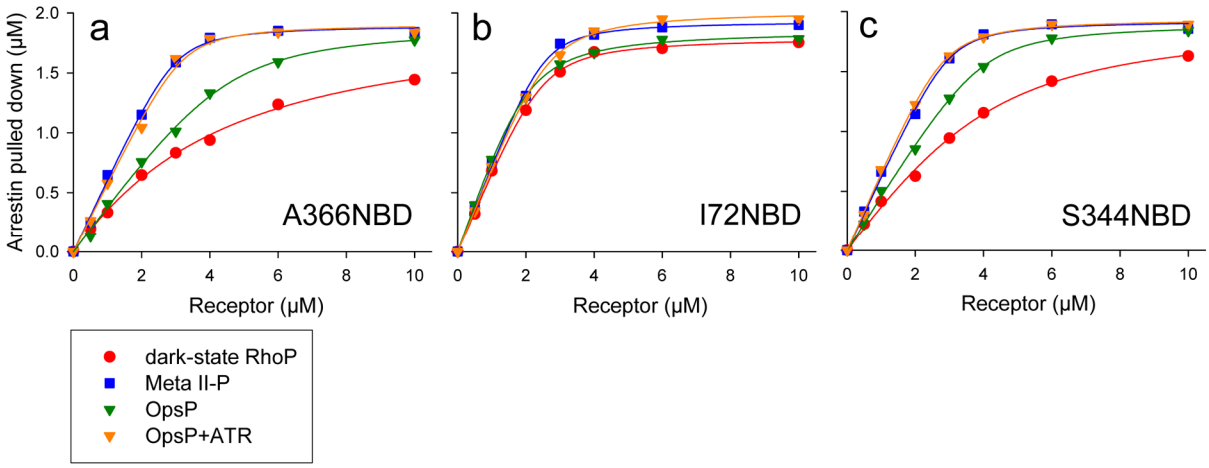

Supplementary Figure S2. Comparison of receptor binding by different NBD-labelled arrestin mutants. Dark-state RhoP (*red*), Meta II-P (*blue*), OpsP (*green*), or OpsP plus a ten-fold excess of all-*trans*-retinal (ATR) (*orange*) were titrated against 2 μM arrestin A366NBD (**a**), I72NBD (**b**), or S344NBD (**c**) in 50 mM HEPES buffer pH 7, and arrestin binding was measured by the centrifugal pull-down assay. Binding curves were fit to data points as described in the *Methods* (Eq. 3). The backside-labelled control, arrestin A366NBD, bound both Meta II-P and OpsP+ATR with high affinity (K_D < 100 nM) and a stoichiometry of about one arrestin per 1.5 receptors. Arrestin A366NBD had lower affinity for OpsP (K_D~400 nM) and relatively poor affinity (K_D>1 μM) for dark-state RhoP. In contrast, arrestin I72NBD bound all forms of phosphorylated receptor with similar affinity and stoichiometry (100 nM < K_D < 200 nM, one arrestin per 1.3 receptors). Arrestin S344NBD was more similar to A366NBD with regard to its relative affinities for different receptor species, although S344NBD bound OpsP and dark-state RhoP with higher affinity than A366NBD. Note that the data in (b) and (c) are also shown in Fig. 6 and are re-plotted here to better show the relative receptor affinities of the different labelled arrestin mutants.

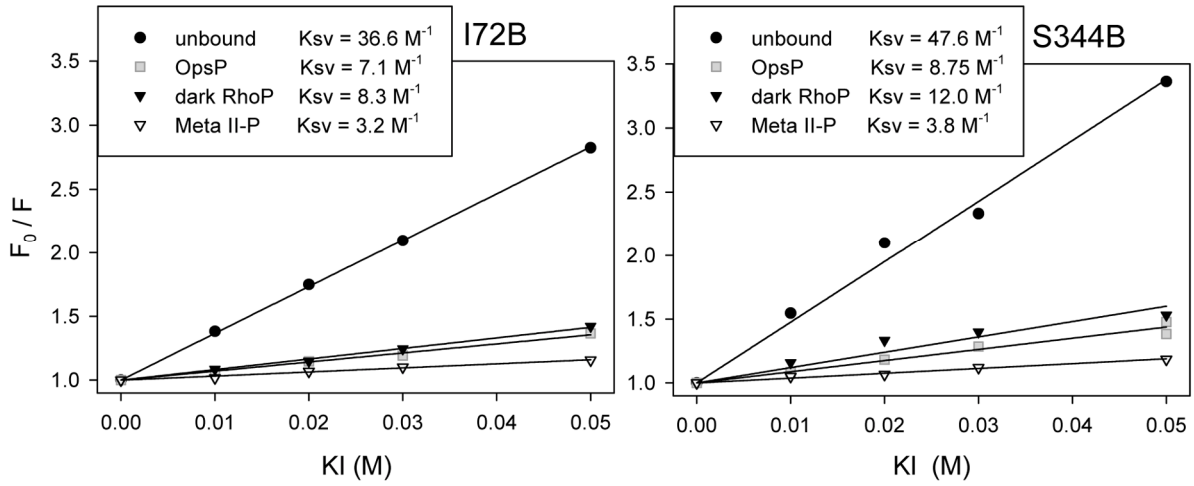

Supplementary Figure S3. Stern-Volmer quenching analysis of bimane-labelled arrestin mutants. We measured the relative accessibility of bimane probes at sites 72 (*left panel*) and 344 (*right panel*) on arrestin to the aqueous quencher iodide as previously described[61]. Briefly, samples contained 2 μM arrestin mutant without or with 20 μM OpsP, dark-state RhoP, or Meta II-P. Fluorescence spectra were taken at increasing KI concentrations, and the total ionic strength was kept constant at 50 mM with KCl. Separate samples were prepared and measured for each KI concentration. Note that bimane-labelled mutants were used, because the short lifetime of NBD makes this probe unsuitable for quenching analysis.

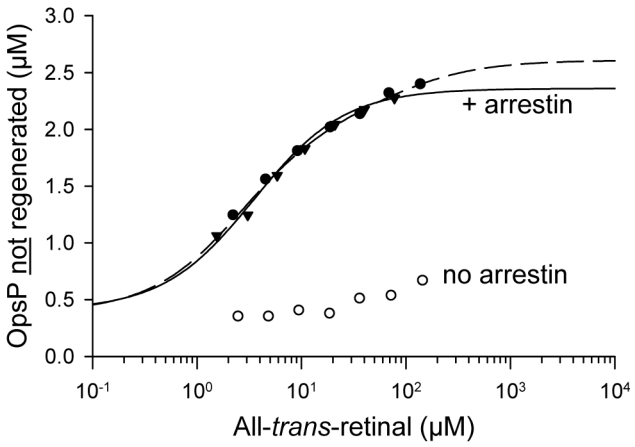

Supplementary Figure S4. High concentrations of ATR alone are not sufficient to block regeneration of rhodopsin. ATR was titrated against 4 μM OpsP in the absence (*open symbols*) or presence (*closed symbols*) of 4 μM arrestin. After equilibration, regeneration with 11-*cis*-retinal was subsequently measured. At high concentrations of ATR, arrestin blocked regeneration in half the OpsP population, while regeneration was minimally affected in the absence of arrestin. The data obtained with arrestin are also shown in Fig. 3a (*green*), and these data were used to fit both single-site (*solid trace*) and two-site (*dashed trace*) binding models.

Supplementary Table S1. Summary of physical parameters for arrestin binding to different phosphorylated receptor species[a]

Receptor species	Apparent K_D (μM)[b]	Stoichiometry (receptors per arrestin)[b]	IC_{50} of NaCl[c] (mM)	IC_{50} of $MgCl_2$[d] (mM)
dark RhoP	*n.d.*[e]	*n.d.*	110	1.5
OpsP	1.5	3.3	110	3.4
Meta II-P	0.31	1.4	1150	138
OpsP + ATR	0.33	1.5	440	32

[a] As determined using the centrifugal pull-down assay.

[b] The combined data points from at least three independent experiments for each receptor species were combined for the curve fitting procedure. Arrestin titrations were performed in isotonic buffer as described in Fig. 2a.

[c] NaCl titration was performed as described in Supplementary Fig. S1a, and data was fit to Supplementary Eq. S1.

[d] $MgCl_2$ titration was performed as described in Supplementary Fig. S1b, and data was fit to Supplementary Eq. S1.

[e] *n.d.* means not determined.

Supplementary Note 1. We probed the chemical nature of the interaction of arrestin with different receptor forms by carrying out salt (NaCl or $MgCl_2$) titrations (Supplementary Fig. S1). Electrostatic interactions are more readily disturbed by salt than hydrophobic interactions. Arrestin binding to either OpsP or dark-state phosphorylated rhodopsin (RhoP) was the most sensitive to salt, with similar IC_{50} values, and arrestin binding to Meta II-P was ~10 times less sensitive to salt (Supplementary Table S1). These results generally agree with those previously published for potassium acetate[62,63], although we found that the divalent Mg^{+2} cation was 10 to a 100-times more effective at disturbing binding than the monovalent Na^{+} cation. Interestingly, the salt sensitivity of arrestin binding to OpsP/ATR was between that of OpsP and Meta II-P. Together these results suggest that arrestin binding to the inactive forms of the receptor (dark-state RhoP[62] and OpsP) is primarily electrostatic in nature. Just as arrestin has a propensity to bind polyanions[64-66], arrestin likely binds RhoP and OpsP by virtue of their highly phosphorylated C-tails. Furthermore, arrestin binding to OpsP/ATR is more like arrestin binding to Meta II-P and involves hydrophobic interactions that are less affected by salt[62]. However, the intermediate sensitivity of the arrestin/OpsP/ATR complex reflects the fact that only half the OpsP population takes up ATR to reform Meta II-P.

Supplementary Note 2. In our recently published study of the arrestin-Meta II-P stoichiometry, we employed rod outer segment membranes in which 70% of receptors were phosphorylated enough to bind arrestin following a flash of light that photo-activated 20% of receptors[67]. With these samples, we consistently measured an arrestin to Meta II-P binding stoichiometry of 1:2 when all receptors were light-activated (Fig. 3d). We further measured arrestin and ATR binding to OpsP derived from these membrane samples (Fig. 3c, d). The data indicated that one arrestin could bind per four receptors in the presence of saturating ATR, and regeneration was blocked in ~30% of the OpsP population. These results suggest that, in preparations where only a fraction of receptors are phosphorylated,

arrestin induces ATR uptake in half of the population that is phosphorylated. In other words, arrestin requires two phosphorylated aporeceptors in order to induce ATR uptake in one aporeceptor. In contrast, arrestin binding to two light-induced Meta II receptors apparently requires only one receptor to be phosphorylated.

Supplementary Note 3. NBD probes at sites 72 and 344 reported no changes in fluorescence when arrestin bound dark-state RhoP (Fig. 6a, e), suggesting these sites were not buried in a hydrophobic environment. Since the fluorescence emission of NBD overlaps with the absorbance of dark-state rhodopsin, it is possible that fluorescence changes were masked by non-radiative energy transfer to the chromophore of rhodopsin. Therefore we further probed the involvement of these sites in arrestin binding of dark-state RhoP by Stern-Volmer quenching analysis[68]. Bimane fluorophores were attached to sites 72 and 344, and the relative solvent accessibility was assessed by titrating iodide[61]. The data indicate that the solvent accessibility of sites 72 and 344 on arrestin decreased about four-fold upon arrestin binding to dark-state RhoP or OpsP (Supplementary Fig. S3). Furthermore, solvent accessibility decreased even more upon light-activation of RhoP to Meta II-P, thus reflecting the tighter interaction of arrestin with Meta II-P as compared to dark RhoP and OpsP. All together, our results suggest that sites 72 and 344, although not deeply buried, are located within the binding interface between arrestin and dark-state RhoP, which is consistent with the observed immobility of spin-labels at these sites under similar experimental conditions[69].

Supplementary Methods

Preparation of Highly Phosphorylated Opsin. The procedure described below is a modified version of one we received from Vsevolod Gurevich (Vanderbilt University, Nashville). All sucrose solutions were prepared in Buffer A (70 mM potassium phosphate, 1 mM $MgCl_2$, 0.1 mM EDTA, pH 7 + 1 mM DTT and 0.5 mM PMSF). The density (ρ) of

each sucrose solution at 4 ℃ was measured with a hydrometer. All procedures were carried out under dim red light. Frozen retina (100) were thawed on ice and then vigorously shaken with 90 mL of ice-cold 45% (w/v) sucrose. The retina suspension was centrifuged at 2,500 x *g* for 5 min. The supernatant was filtered through several layers of cheesecloth and then diluted slowly 1:1 with ice-cold Buffer A. This suspension was centrifuged at 6,000 x *g* for 7 min. The supernatant was carefully poured off and the pellets were gently resuspended in 25.5% sucrose (ρ=1.105 g/mL). This suspension (40 mL) was then layered onto four gradients composed of 14 mL 32.25% sucrose (ρ=1.135 g/mL) overlaid with 14 mL 27.125% sucrose (ρ=1.115 g/mL). The gradients were centrifuged at 25,000 rpm (Beckman SW 28 rotor) for 30 min using slow acceleration and deceleration settings. The ROS localized to the interface between the 27.125% and 32.25% solutions, and bands were collected by puncturing the tube with a needle coupled to a syringe. The ROS were then diluted 1:1 with ROS buffer and centrifuged at 48,000 x *g* for 30 min. The ROS pellets were resuspended in ~10 mL of ROS buffer, snap frozen in liquid N_2, and stored wrapped in aluminium foil at -80 ℃.

The ROS suspension was later thawed and homogenized in 40 mL of Buffer B (100 mM potassium phosphate pH 7.4) using an all-glass douncer in dark conditions. The homogenized ROS was diluted with Buffer B to a final volume of 100 mL, 10 µM of 11-*cis*-retinal was added, and the ROS were incubated at room temperature for 15 min. A concentrated stock of ATP (400 mM) was freshly prepared in Buffer B and then added to the ROS suspensions at a final concentration of 8 mM ATP. 2 mM $MgCl_2$ was also added from a 1 M stock solution. Sealed transparent tubes of this ROS suspension were placed on a rocking platform ~50 cm under a standard desk lamp at room temperature (22 - 23 ℃). After two hours, 20 mM NH_2OH from a 1M stock (pH 7) was added in order to convert all rhodopsin photoproducts to opsin and retinal oxime. After 15 minutes, the phosphorylated opsin (OpsP) suspension was diluted 1:3 with cold buffer B and

centrifuged at 48,000 x *g* for 30 min. The OpsP was then washed by resuspending in 40 mL Buffer B, homogenizing using a glass douncer, diluting 1:8 with Buffer B, and then centrifuging again at 48,000 x *g* for 30 min. The OpsP was then washed in a similar manner using 50 mM HEPES buffer pH 7. Finally, the membrane pellets were resuspended and homogenized in 50 mM HEPES buffer pH 7at a final OpsP concentration of 100 - 200 μM. The final yield was usually 30 to 50 mg of phosphorylated opsin from 100 retinas. The membrane suspension was aliquoted, snap frozen in liquid N_2, and stored at -80 ℃.

An absorbance spectrum of our OpsP preparation solubilized in 1% dodecyl-β-D-maltoside showed that all-*trans*-retinal-oxime (360 nm) was present at one to two-fold molar excess. The concentration of OpsP was determined by regenerating a small aliquot with a 5-fold molar excess of 11-*cis*-retinal for one hour at room temperature and subsequently measuring the absorbance of a 1:20 dilution in 100 mM hydroxylamine (pH 7). The loss of 500 nm absorbance after illumination corresponded to the rhodopsin, and hence OpsP, concentration ($\varepsilon = 0.0408\ \mu M^{-1}cm^{-1}$)[67].

Note that, in contrast to our previously published protocols[61,67], the OpsP membranes used in this study were not extensively washed with BSA to remove excess retinal oxime. We recently discovered that this procedure decreased the phosphorylation level of the preparation. Since retinal oxime does not bind opsin, the retinal oxime present in our samples is not expected to affect the results presented in our study. In addition, our washing procedure was sufficient to remove the soluble and membrane-associated proteins present in ROS (*e.g.* transducin and arrestin), as evidenced by SDS PAGE and a lack of “Extra Meta II” for washed ROS membranes alone (Fig. 1).

For experiments requiring rhodopsin, 11-*cis*-retinal was added in three-fold molar excess to membranes containing OpsP. After one hour at room temperature, 20 mM hydroxylamine was added, and the membranes were subsequently centrifuged and

washed three times with buffer. Rhodopsin concentration was determined by difference spectrum as described[67].

Mathematical Analysis of Salt Titration Curves. Salt titration data were fit to a dose-response curve, where *min* is the minimal value, *max* is the maximal value, IC_{50} is the half maximal inhibitory concentration, and *H* is the Hill coefficient that describes the slope of the curve.

$$y = \min + \frac{\max - \min}{1 + \left(\frac{x}{IC_{50}} \right)^{H}} \qquad \text{(S1)}$$

The graphing program SigmaPlot 10.0 was used to fit experimental data using nonlinear regression algorithms.

Supplementary References

61. Sommer, M.E., Smith, W.C. & Farrens, D.L. Dynamics of arrestin-rhodopsin interactions: arrestin and retinal release are directly linked events. *J Biol Chem* **280,** 6861-71 (2005).
62. Gurevich, V.V. & Benovic, J.L. Visual arrestin interaction with rhodopsin. Sequential multisite binding ensures strict selectivity toward light-activated phosphorylated rhodopsin. *J Biol Chem* **268,** 11628-38 (1993).
63. Vishnivetskiy, S.A. et al. Regulation of arrestin binding by rhodopsin phosphorylation level. *J Biol Chem* **282,** 32075-83 (2007).
64. Palczewski, K., Pulvermüller, A., Buczylko, J., Gutmann, C. & Hofmann, K.P. Binding of inositol phosphates to arrestin. *FEBS Lett* **295,** 195-9 (1991).
65. Palczewski, K., Pulvermüller, A., Buczylko, J. & Hofmann, K.P. Phosphorylated rhodopsin and heparin induce similar conformational changes in arrestin. *J Biol Chem* **266,** 18649-54 (1991).
66. Wilson, C.J. & Copeland, R.A. Spectroscopic characterization of arrestin interactions with competitive ligands: study of heparin and phytic acid binding. *J Protein Chem* **16,** 755-63 (1997).
67. Sommer, M.E., Hofmann, K.P. & Heck, M. Arrestin-rhodopsin binding stoichiometry in isolated rod outer segment membranes depends on the percentage of activated receptors. *J Biol Chem* **286,** 7359-69 (2011).
68. Lakowicz, J.R. *Principles of Fluorescence Spectroscopy*, (Kluwer Academic, New York, 1999).
69. Hanson, S.M. et al. Differential interaction of spin-labeled arrestin with inactive and active phosphorhodopsin. *Proc Natl Acad Sci U S A* **103,** 4900-5 (2006).